MTOpen

Adeno-associated Virus–mediated Delivery of a Recombinant Single-chain Antibody Against Misfolded Superoxide Dismutase for Treatment of Amyotrophic Lateral Sclerosis

Priyanka Patel[1,2], Jasna Kriz[1,2], Mathieu Gravel[1,2], Geneviève Soucy[1,2], Christine Bareil[1,2], Claude Gravel[1,2] and Jean-Pierre Julien[1,2]

[1]Research Centre of Institut universitaire en santé mentale de Québec, Québec, Québec, Canada; [2]Department of Psychiatry and Neuroscience, Laval University, Québec, Québec, Canada

There is emerging evidence that the misfolding of superoxide dismutase 1 (SOD1) may represent a common pathogenic event in both familial and sporadic amyotrophic lateral sclerosis (ALS). To reduce the burden of misfolded SOD1 species in the nervous system, we have tested a novel therapeutic approach based on adeno-associated virus (AAV)–mediated tonic expression of a DNA construct encoding a secretable single-chain fragment variable (scFv) antibody composed of the variable heavy and light chain regions of a monoclonal antibody (D3H5) binding specifically to misfolded SOD1. A single intrathecal injection of the AAV encoding the single-chain antibody in SOD1^{G93A} mice at 45 days of age resulted in sustained expression of single-chain antibodies in the spinal cord, and it delayed disease onset and extension of life span by up to 28%, in direct correlation with scFv titers in the spinal cord. The treatment caused attenuation of neuronal stress signals and reduction in levels of misfolded SOD1 in the spinal cord of SOD1^{G93A} mice. From these results, we propose that an immunotherapy based on intrathecal inoculation of AAV encoding a secretable scFv against misfolded SOD1 should be considered as potential treatment for ALS, especially for individuals carrying SOD1 mutations.

Received 21 August 2013; accepted 7 October 2013; advance online publication 7 January 2014. doi:10.1038/mt.2013.239

INTRODUCTION

Amyotrophic lateral sclerosis (ALS) is an adult-onset neurodegenerative disorder characterized by the selective loss of upper and lower motor neurons.[1] Approximately 20% of familial ALS cases are caused by mutations in the Cu/Zn superoxide dismutase 1 (SOD1).[2–4] Although the mechanism by which SOD1 mutations cause selective degeneration of motor neurons is not fully understood, many lines of evidence suggest that the toxicity of mutant SOD1 is related to its propensity to misfold and to aggregate.[5,6] Furthermore, some studies suggest a possible involvement of SOD1 abnormalities in sporadic ALS cases with no SOD1 mutations.[7–11] For instance, oxidation of wild-type (WT) SOD1 generates misfolded proteins that may acquire the binding and toxic properties of mutant SOD1.[7,10]

The finding that mutant SOD1 can be secreted and evidence of toxicity of extracellular mutant SOD1[12] provided a rationale for testing immunization approaches for ALS treatment. An active immunization approach with recombinant mutant or WT SOD1 as immunogen was found to delay disease onset and to increase life span of SOD1^{G37R} mice and SOD1^{G93A} mice expressing moderate levels of mutant SOD1.[13,14] Similar results have been obtained with active immunization using an antigenic peptide that targets the dimer interface of SOD1 using SOD1^{G37R} or SOD1^{G93A} mice.[15] However, because of potential adverse effects of immune responses to active vaccination approaches, passive immunization strategies appear more appropriate for future human ALS clinical trials. Some monoclonal antibodies recognizing the misfolded forms of SOD1 have been tested in SOD1^{G93A} mice.[16] Intracerebroventricular injection of one of those monoclonal antibodies in SOD1^{G93A} mice, named the D3H5 antibody, caused reduction in levels of misfolded SOD1 in the spinal cord and prolonged the life span of SOD1^{G93A} mice in relation to duration of treatment. The monoclonal D3H5 antibody was shown to react against various human SOD1 mutants besides SOD1 G93A, including SOD1 G37R, G127X, G85R, and D90A.[16] In addition, the D3H5 antibody also detected WT SOD1 after treatment with metal chelators that induce protein misfolding.[16] So, the D3H5 antibody acts as a probe for SOD1 misfolding whether it is caused by mutations or other alterations such as copper or zinc depletion. The activity of D3H5 antibody against central nervous system (CNS) tissue from sporadic cases of ALS remains to be investigated.

Interestingly, intracerebroventricular injection of the variable Fab fragment of the same anti-SOD1 antibody (D3H5) also slowed down disease in SOD1^{G93A} mice, raising the possibility to engineer a single-chain fragment of variable regions from this antibody to neutralize the toxicity of misfolded SOD1. Such single-chain fragment variable (scFv) antibody should offer some advantages such as small size and low immunogenicity. Moreover, scFv

Correspondence: Jean-Pierre Julien, Research Centre of Institut universitaire en santé mentale de Québec, 2601 Chemin de la Canardière Québec, Québec G1J 2G3, Canada (E-mail: jean-pierre.julien@fmed.ulaval.ca)

antibodies can be used in gene delivery systems. Recombinant adeno-associated viruses (AAVs) are presently vehicles of choice for gene transfer in the nervous system.[17] AAV vectors provide stable and safe gene expression with minimal immune responses and broad cell type tropism. In recent years, AAV has been used successfully for gene delivery in treatment of human genetic disorders, especially in retinal disease.[18] When injected into the cerebrospinal fluid (CSF), AAV vectors were reported to confer widespread and sustained transgene expression in the CNS.[19]

Here, we report the generation an AAV vector encoding a secretable scFv antibody (AAV-scFv) to target misfolded SOD1. A single intrathecal injection of this AAV viral vector in adult SOD1^{G93A} mice led to sustained production of secretable scFv antibodies in the spinal cord, and it significantly delayed disease onset and mortality. This therapeutic approach may be applicable to ALS cases with SOD1 mutations and perhaps to subset of sporadic ALS cases given that misfolded and aggregated SOD1 species have been detected in sporadic ALS[7–11]

RESULTS

Generation of a scFv from the D3H5 hybridoma

Based on our finding that the Fc region of mAbD3H5 was dispensable for extending the survival of transgenic SOD1^{G93A} mice when delivered into the CSF,[16] we planned to test whether tonic delivery of the binding domain of the antibody via virus-mediated gene transfer in the spinal cord would be effective in blocking the toxicity of misfolded human SOD1. Thus, a scFv-encoding plasmid was generated by cloning and assembly of the coding sequences of the variable immunoglobulin heavy and light chains of mAbD3H5 into a single open-reading frame encoding a hybrid protein bearing both variable immunoglobulin regions attached by a short flexible peptide linker. The DNA sequences and deduced amino acid sequences of the cloned hypervariable regions of mAbD3H5 light and heavy chains are shown in **Figure 1a**.

The scFv DNA construct was subcloned into an expression vector under the control of cytomegalovirus (CMV) promoter that provided a murine immunoglobulin (Ig) κ-secretory signal and a human c-myc epitope to facilitate detection. We analyzed the expression of scFvD3H5 after DNA transfection in HEK293T (human embryonic kidney cell line) cells by western blotting and enzyme-linked immunosorbent assay (ELISA). The scFv was detected in the 1% Triton cell lysate and in the conditioned media after transient transfection in HEK293T cells (**Figure 1b**). A 28-kDa band was detected by immunoblotting after sodium dodecyl sulfate-polyacrylamide gel electrophoresis (SDS-PAGE) using an antibody against the human c-myc tag in the recombinant scFv protein. To test whether the scFvD3H5 antibody was able to detect misfolded SOD1, we used conditioned media from cells transiently transfected with the D3H5scFv encoding plasmid as a primary antibody source for immunoblotting detection after SDS-PAGE of spinal cord lysate from SOD1^{G93A} mice. The scFvD3H5 in the media detected specifically SOD1 species by immunoblotting as revealed by an anti-myc antibody, whereas no signal was seen with conditioned medium from mock-transfected cells (**Figure 1c**). In addition, when conditioned media containing scFvD3H5 antibodies was loaded on ELISA plate coated with recombinant human SOD1, the bound scFvD3H5 protein could be detected using HRP conjugated anti-myc (**Figure 1d**).

AAV-mediated transduction of scFv anti-SOD1 in the spinal cord of SOD1^{G93A} mice

As described in Methods, we then generated an AAV viral vector encoding the secretable scFvD3H5 protein. To test the therapeutic effect of scFvD3H5 in ALS pathogenesis, single intrathecal injection of 3×10^9 particles of the AAV 2/1 encoding scFvD3H5 was carried out in SOD1^{G93A} mice at 45 days of age. At 5 weeks after injection, spinal cord sections were examined by immunostaining using an anti-myc antibody for detection of scFvD3H5. Robust scFvD3H5 immunostaining was observed in the ventral spinal cord of lumbar and sacral regions. The scFvD3H5 antibody was detectable over an extensive portion of the spinal cord. Double immunostaining was also performed using anti-myc tag and anti-choline acetyltransferase (ChAT) antibodies. The myc tag immunoreactivity was detected in some of the ChAT-positive cells in ventral horn spinal cord of SOD1^{G93A} mice injected with AAV-scFvD3H5 (**Figure 2a**,**b**). No staining was detected in vehicle-injected SOD1^{G93A} mice. The myc ta0 days or more after AAV injection), indicating a stable transduction of scFvD3H5 by AAV-infected cells in SOD1^{G93A} mice (**Figure 2c**,**d**). The presence of scFvD3H5 antibody in the spinal cord was also confirmed by immunoprecipitation of scFvD3H5 antibody from total spinal cord lysate using a monoclonal anti-c-myc as described previously[20] and then by detection of immunoprecipitated protein on immunoblot after SDS-PAGE with a second polyclonal anti-c-myc by immunoblotting. The immunoblots further confirmed the presence of scFvD3H5 in the spinal cord at 5 weeks postinjection of AAV-scFvD3H5 in SOD1^{G93A} mice (**Figure 2e**).

One potential concern associated with AAV-mediated gene delivery is the host immune response. To investigate any possible immune response of AAV-scFvD3H5 into mice, we took advantage of a TLR2-LUC-AcGFP (Toll like receptor 2–luciferase Aequorea coerulescens green fluorescent protein) mouse model where transcriptional activation of TLR2 as reporter of inflammation can be visualized in live animals using biophotonic molecular imaging.[21] Single intraperitoneal injection of lipopolysaccharide (LPS) at a rate of 5 mg/kg in mice induced a strong induction of bioluminescense signal in spinal cord after 24 hours (**Supplementary Figure S1A–C**). We injected intrathecally 3×10^9 particles of the AAV 2/1 encoding scFvD3H5 or same amount of saline in TLR2-LUC-AcGFP mice. Live imaging of the spinal cord of injected mice was carried out by up to 3 weeks. Our imaging analysis did not reveal induction of inflammatory response after intrathecal injection of AAV-scFvD3H5, control virus AAV-scFvD1.3 (AAV encoding lysozyme specific single chain fragment D1.3) in TLR2-LUC-AcGFP transgenic mice (**Supplementary Figure S1D–J**).

Single intrathecal injection of AAV-scFvD3H5 delayed disease onset and increased life span of SOD1^{G93A} mice

We examined the effects on life span of SOD1^{G93A} mice of a single intrathecal injection of AAV-scFvD3H5 and vehicle at 45 days of age. AAV-scFvD3H5–injected mice had a significant extension of

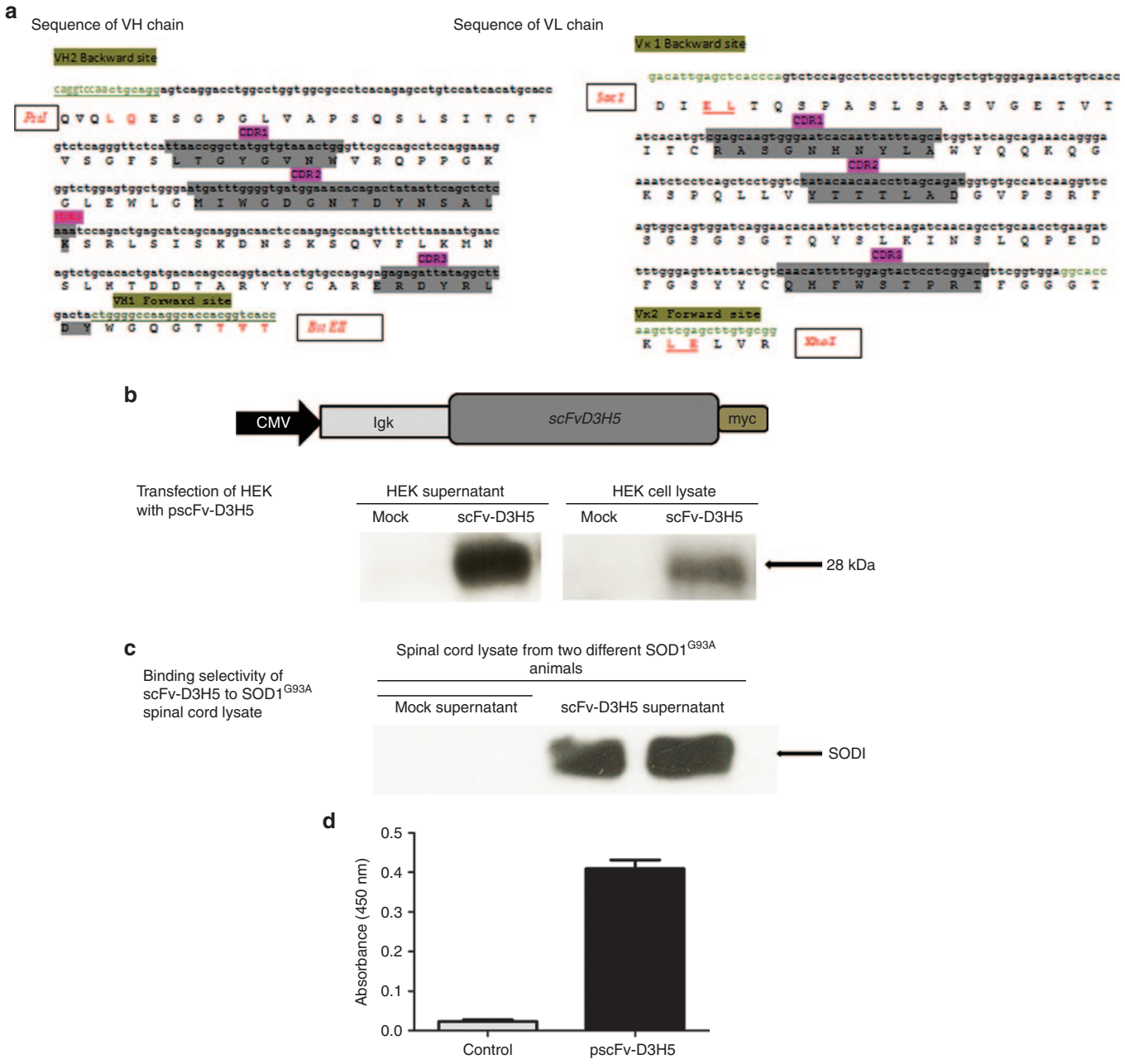

Figure 1. Generation of recombinant single-chain fragment variable (scFv) antibody against misfolded superoxide dismutase 1 (SOD1). (**a**) Nucleotide and deduced amino acid sequences for the scFv heavy chain variable (VH) and light chain variable (VL) are shown along with complementarity-determining regions and positions of restriction sites for enzymes and primers. (**b**) A cytomegalovirus (CMV) enhancer containing promoter drives the expression of scFv, which harbors an amino terminal immunoglobulin (Igκ) secretory signal and carboxy-terminal human c-myc epitope. pscFv-D3H5 was transiently transfected into HEK cells, and mock-transfected HEK cells (without any vector plasmid) was used as a control. Culture media (CM) was harvested 48 hours following transfection. Conditioned media and 1% Triton lysate was analyzed by western blot, detected with anti c-myc, showing expression of anti-mSOD1scFv. (**c**) Secreted scFv antibodies in conditioned media from transfected HEK cells were used as primary antibodies source to probe $SOD1^{G93A}$ spinal cord lysates by western blot, showing binding selectivity of scFvD3H5. (**d**) Ninety-six well plates were coated with recombinant G93A polypeptide and the harvested CM containing scFvD3H5 was subsequently added to well. Unbound proteins were washed away, and anti-myc-HRP antibody was used to detect the scFv that remained bound to well. An unpaired *t*-test was performed to determine significant differences ($P < 0.0001$).

life span by an average of 16 days (P value of 0.0001, median survival of 159 days) when compared with $SOD1^{G93A}$ mice injected with vehicle and AAV scFvD1.3 (median survival of 143 days; **Figure 3a**). No adverse effect or premature death occurred in normal non-transgenic mice injected with AAV-scFvD3H5. Moreover, the administration of AAV-scFvD3H5 significantly delayed the onset of disease as assessed by rotarod performance tests, reflex score, and body weight, compared with control virus AAV-scFvD1.3– or vehicle-injected $SOD1^{G93A}$ mice (**Figure 3b–d**). Rotarod tests demonstrated that AAV-scFvD3H5–treated $SOD1^{G93A}$ animals maintained their ability to coordinate their movement for a longer period than both the control group animals from 110 days of

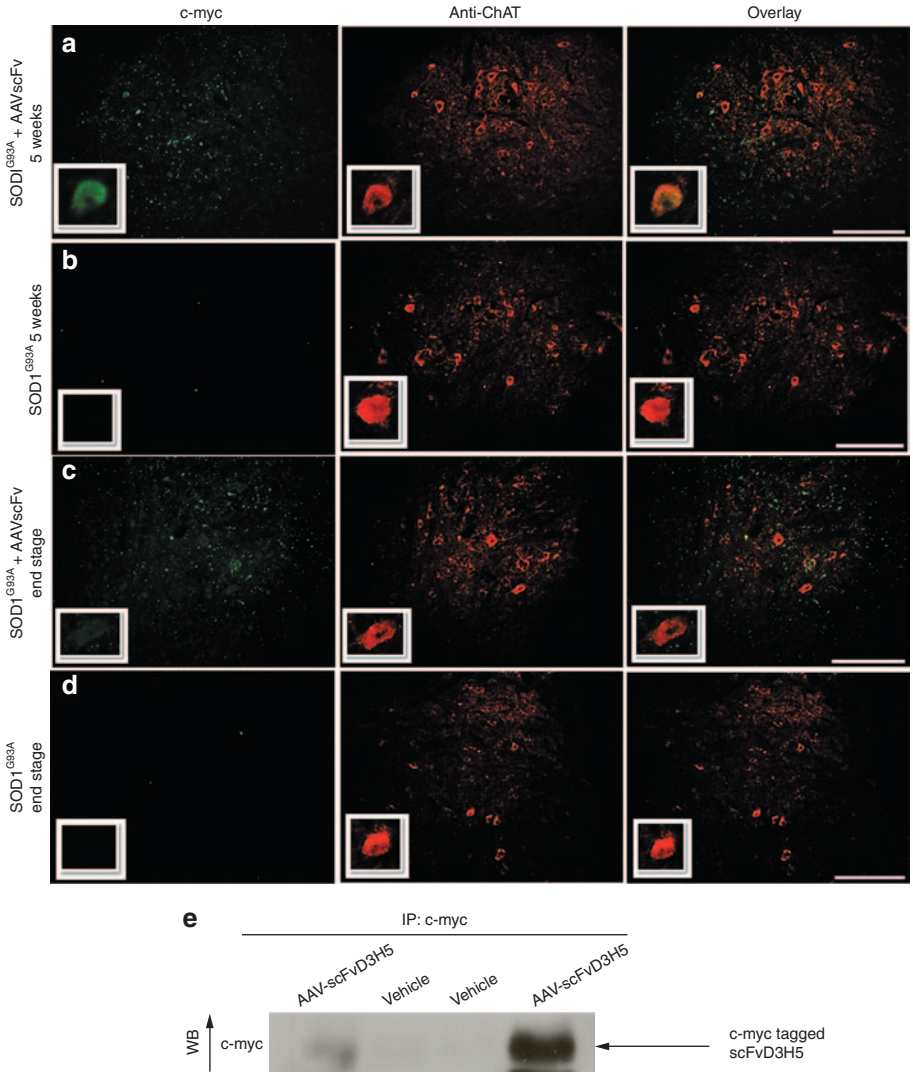

Figure 2. Immunodetection of single-chain fragment variable (scFv) antibody with anti-myc antibody in spinal cord of SOD1^{G93A} mice. Postnatal day 45 mice were intrathecally injected with AAV-scFvD3H5. The presence of the scFv protein was visualized with antibodies recognizing the human c-myc tag present in the protein in spinal cord tissues collected 5 weeks after injection of the viral vector, or at the end point of mice (100 days or more after injection). (**a**,**c**) Myc tag immunoreactivity was widely distributed in spinal cord sections at both 5 weeks and much later at the mice end stage. Double immunofluorescence staining with anti-ChAT and anti-c-myc tag antibodies reveals colocalization of myc tag and ChAT immunoreactivities in some motor neurons of spinal cord ventral horn of AAV-scFvD3H5–injected mice (anti-c-myc and ChAT colocalization is shown in inlay magnification of a representative cell in the boxed panel). (**b**,**d**) No myc tag immunoreactivity was seen in control mice scale bar 50 µm. (**e**) Immunoprecipitation (IP) from tissue expressing scFvD3H5. The spinal cord of AAV-scFvD3H5–injected mice was harvested at 5 weeks after delivery, homogenized, and immunoprecipitated with an anti-human myc monoclonal antibody. A second anti-myc polyclonal antibody was used for western blotting. Immunoprecipitates from different samples were loaded in each well. AAV, adeno-associated virus; ChAT, choline acetyltransferase; SOD1, superoxide dismutase 1; WB, western blot.

age onward until end stage ($P < 0.05$ from 110 days of age onward; $n = 10$ animals/group) (Figure 3b). In addition, reflex score measurements demonstrated that AAV-scFvD3H5–treated animals maintained significantly ($P < 0.05$) higher reflex of hind limb from 106 to 135 days of age when compared with those animals having received AAVscFvD1.3 or vehicle injection (Figure 3c). Body weight measurements revealed a significantly slower loss of body weight in AAV-scFvD3H5–treated transgenic mice from 113 to 127 days ($P < 0.05$) (Figure 3d). The mean delay in the combined assessments for rotarod test and body weight was 15 days. In all motor function tests, there was no difference between vehicle-treated controls and AAV-scFvD1.3–treated SOD1^{G93A} mice.

Correlation between scFvD3H5 titer and longevity of SOD1^{G93A} mice

Remarkably, a single intrathecal injection of AAV-scFvD3H5 increased the life span of SOD1^{G93A} mice by up to 40 days (up to 28%). However, there was a large variation in the survival of transgenic mice injected with AAV-scFvD3H5, which is likely due to technical difficulty in achieving consistent viral delivery via intrathecal injection in mice. This led us to assess the antibody titer of the scFvD3H5 protein in the spinal cord at end stage of disease in these mice. Again, we took advantage of the presence of the human c-myc tag on the protein to design ELISA test for dosing scFvD3H5 proteins in spinal cord lysates

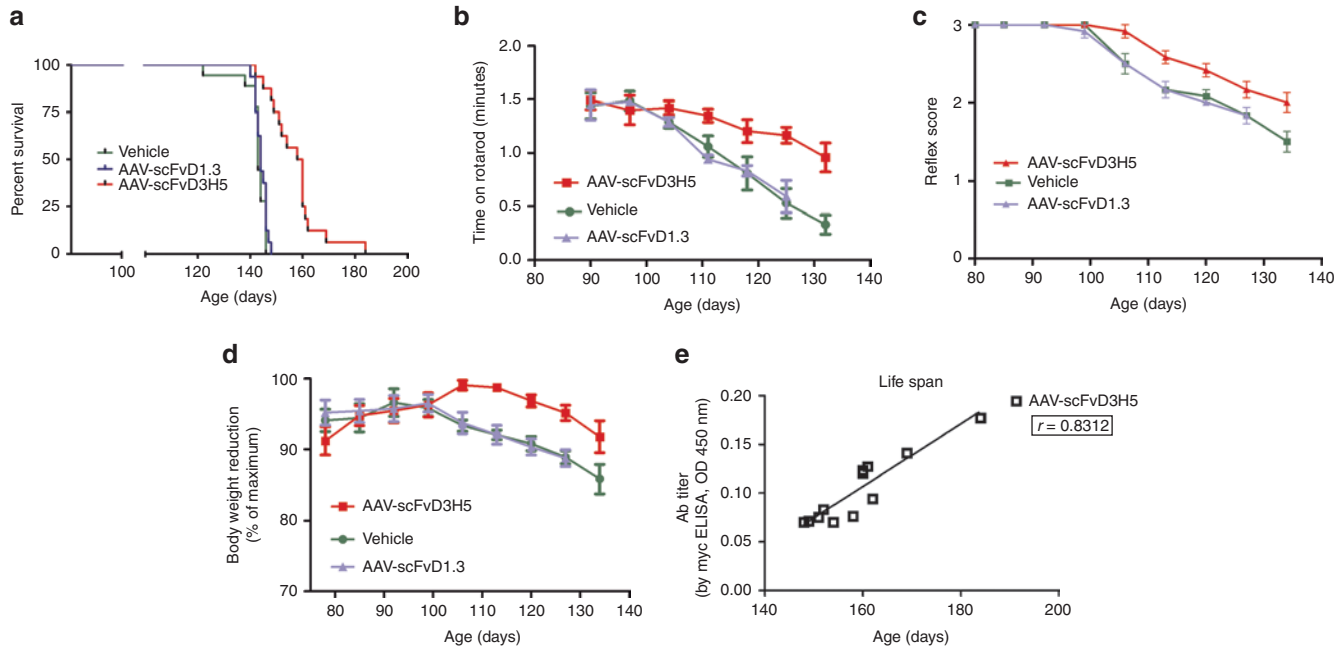

Figure 3. Delayed disease onset and extension of life span in AAV-scFvD3H5 treated SOD1^{G93A} mice. (**a**) Intrathecal administration of AAV-scFvD3H5 increased the life span of SOD1^{G93A} mice. Kaplan–Meier curve for survival is shown (n = 16 for AAV-scFvD3H5–treated SOD1^{G93A} mice and n = 18 for vehicle-treated SOD1^{G93A} mice, $P < 0.0001$ by log-rank test). (**b**) Rotarod test: the time on rotarod was determined for SOD1^{G93A} mice injected with AAV-scFvD3H5, AAV-scFvD1.3, and with vehicle (n = 6 for all). AAV-scFvD3H5 treatment significantly improved motor performance ($P < 0.001$ by *post hoc* test) when compared with AAVscFvD1.3– or vehicle–administered mice. Each point indicates average ± SEM. Moreover, AAV-scFvD3H5 injection delays onset as defined by (**c**) prolonged maintenance of reflex score in the treated mice and (**d**) reduction in body weight loss ($P < 0.05$) AAV-scFvD3H5–treated mice are shown in red, AAVscFvD1.3–treated mice are shown in blue, and vehicle-treated mice are shown in green. (**e**) Antibody titer positively correlated with life span of AAV-scFvD3H5–injected mice. ELISA for c-myc tag in spinal cord lysates from AAV-scFvD3H5–injected mice (end stage) was carried out to measure scFv titers. Absorbance (450 nm) from ELISA for c-myc tag and life span was plotted on a scatter diagram, shows a direct correlation of titer and longevity ($P < 0.0001$ and Spearman r = 0.8312). AAV, adeno-associated virus; Ab, antibody; scFv, single-chain fragment variable; SOD1, superoxide dismutase 1.

of treated SOD1^{G93A} mice. We found that the survival time of SOD1^{G93A} mice directly correlated with the titer of scFvD3H5 protein in spinal cord extract at end stage of disease (r = 0.8312; $P < 0.0001$) (**Figure 3e**). The mice that survived for the longest time showed higher titers of scFvD3H5 in their spinal cord tissues.

SOD1^{G93A}–mediated disease is associated with onset of early neuronal stress

Synthesis of mutant SOD1 within motor neurons has been found to be a primary determinant of early neuronal stress, disease onset, and motor neuron injury.[22] To visualize these events from live animals and to analyze the effects of treatment of SOD1^{G93A} with scFvD3H5 on neuronal stress in real time, we took advantage of the GAP-43-luc/gfp reporter mice recently generated and validated in our laboratory.[23] Recent studies using laser capture dissection and gene array analysis revealed that GAP-43 is upregulated in the motor neurons of SOD1^{G93A} mice in the presymptomatic and early symptomatic stage of disease[24], suggesting that GAP-43 may represent a good biomarker to visualize early neuronal stress/damage in ALS mice. Double-transgenic GAP-43-luc/gfp;SOD1^{G93A} mice were generated by crossing heterozygous mice carrying the mutant SOD1^{G93A} transgene with the heterozygous GAP-43-luc/gfp mice coexpressing reporter transgene, luciferase (luc) and green fluorescent protein (gfp), driven by the murine GAP-43 promoter. In this mouse model, a GAP-43 upregulation (luciferase expression detectable as a bioluminescence/photon emission and gfp expression detectable by confocal microscopy) can be followed longitudinally in live animals using bioluminescence/biophotonic imaging and a high-sensitivity/high-resolution charge-coupled device camera (**Figure 4a**). The quantitative analysis of biophotonic signals revealed significant early and presymptomatic upregulation of the GAP-43 signals starting at 8 weeks/56 days and reaching the peak at 11 weeks/77 days of age in the spinal cord of SOD1^{G93A} mutant mice when compared with WT littermates (**Supplementary Figure S2A**). Fluorescence microscopy of gfp and anti-NeuN has been carried out to identify neurons as being the cells expressing induced GAP-43-luc/gfp transgene (**Supplementary Figure S2B**). Furthermore, as previously reported,[22] the ATF3 is upregulated in spinal motor neurons of SOD1^{G93A} mice (**Figure 4b**). The detection of ATF3 in gfp-positive motor neurons in the spinal cord sections of GAP-43-luc/gfp/SOD1^{G93A} mice further confirmed the validity of the GAP-43-luc/gfp transgene for live analysis of neuronal stress in this mouse model (**Figure 4b**).

AAV-scFvD3H5 treatment reduces neuronal stress

Series of live imaging experiments and quantification of signals in GAP-43-luc/gfp;SOD1^{G93A} mice injected with AAV-scFvD3H5 or vehicle revealed that scFvD3H5 expression resulted in a significantly weaker bioluminescence signal in the spinal cord at 5 and

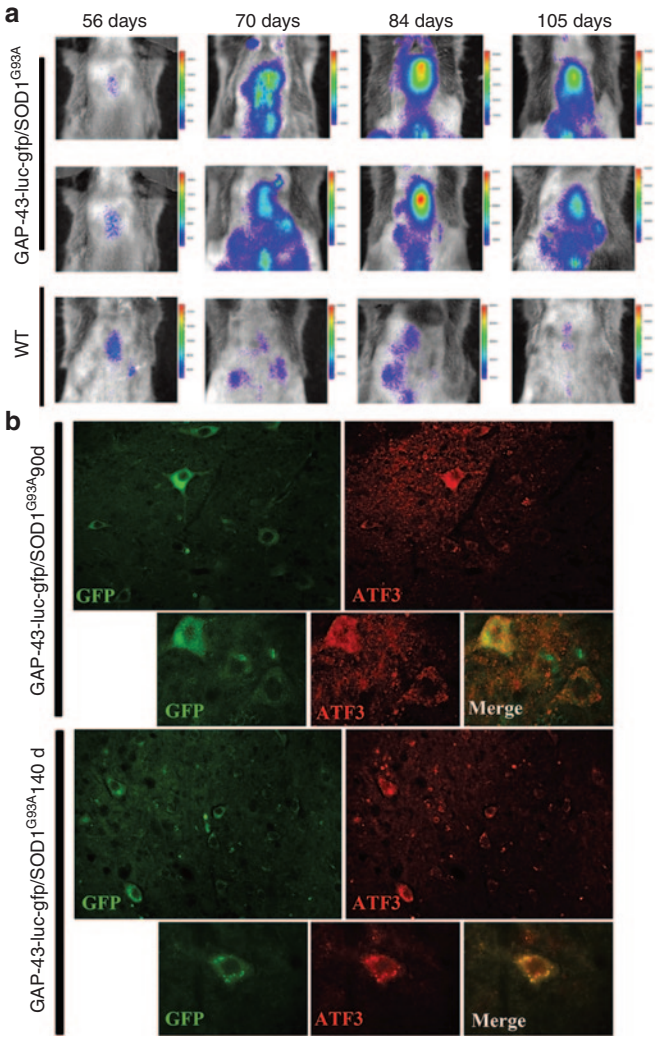

Figure 4. GAP-43-luc-gfp;SOD1^{G93A} double-transgenic mice as a model for live imaging of neuronal stress. (**a**) Representative images of *in vivo* bioluminescence imaging of spinal cord of GAP-43-luc-gfp/SOD1^{G93A} mice and wild-type (WT) mice at various time points, which shows the GAP-43 signal intensity as a measure of neuronal damage. (**b**) Representative immunofluorescence images of spinal cord sections of double-transgenic mice showing colocalization of green fluorescent protein (GFP) and activating transcription factor 3 (ATF3) at lower and higher magnifications. scFv, single-chain fragment variable; SOD1, superoxide dismutase 1.

6 weeks after injection (11 and 12 weeks of age) compared with vehicle-treated double-transgenic mice (Figure 5a,b). The reduction of neuronal stress in mice was further confirmed by examination of spinal cord sections from AAV-scFvD3H5–treated and untreated SOD1^{G93A} mice after immunofluorescence processing to detect the presence of cyclic AMP-dependent transcription factor activating transcription factor 3(ATF3), a marker for neuronal stress[25] (Figure 5c). Thus, the ATF3-like immunofluorescence was much weaker in the spinal neurons of scFvD3H5-treated SOD1^{G93A} mice at 6 weeks after injection as compared with that of untreated mice. The combined data from GAP-43-luc/gfp transgene and ATF3 expression signals demonstrate that treatment with AAV-scFvD3H5 reduced the neuronal stress associated with ALS pathogenesis in SOD1^{G93A} mice.

Alleviation of gliosis and reduction in burden of misfolded SOD1

In addition to motor neuron loss, gliosis in the spinal cord is a prominent pathological feature in ALS patients and in rodent models of ALS.[26,27] Reactive astrocytes and microglia are characterized by an upregulation of Iba1 (Ionized calcium binding adaptor molecule 1) and of GFAP (glial fibrillary acidic protein) in the disease process.[26] We therefore examined the effect of scFvD3H5 treatment on microglial and astroglial activation in SOD1^{G93A} mice at 120 days of age. As shown in Figure 6a,b, Iba 1 immunofluorescence in spinal cord samples from scFvD3H5-treated mice was 29% lower than in control samples (significant difference, $P = 0.0438$). Similarly, astrocyte reactivity as determined by GFAP immunodetection was 38% weaker in SOD1^{G93A} mice injected with AAV-scFvD3H5, also a statistically significant difference ($P = 0.0369$) (Figure 6c,d).

To examine the effect of scFvD3H5 treatment on the levels of misfolded SOD1 species in affected tissues, we carried out immunoprecipitation of misfolded SOD1 from total spinal cord extract at postnatal day 120, using the anti-misfolded SOD1-specific B8H10 antibody[16] followed by SDS-PAGE and immunoblotting using a polyclonal anti-SOD1 antibody. The immunoblots revealed a 19% reduction ($P = 0.0293$) in the levels of misfolded SOD1 species immunoprecipitated by the B8H10 antibody from spinal cord extracts of AAV-scFvD3H5–injected SOD1^{G93A} mice in comparison with the levels detected in vehicle-injected SOD1^{G93A} mice (Figure 6e,f). In addition, comparison of immunoreactivity scores of spinal cord sections measured by fluorescence microscopy revealed marked reduction of anti-misfolded SOD1 antibody signals (B8H10 and C4F6) from samples of AAV-scFvD3H5–injected mice when compared with controls ($n = 3$; $P = 0.01$) (Figure 6g,h). From these results, we conclude that the AAV-mediated delivery of scFvD3H5 antibodies succeeded in reducing the levels of misfolded SOD1.

Attenuation of motor neuron loss in SOD1^{G93A} mice injected with AAV-scFvD3H5

Motor neuron loss correlates with disease severity in transgenic mice expressing mutant SOD1.[2] Therefore, we investigated the effect of the scFvD3H5 treatment on motor neuron survival in SOD1^{G93A} mice by quantitative evaluation of the number of large Nissl-positive neurons in the ventral horn region of lumber spinal cord sections (Figure 7a). At 120 days of age, the SOD1^{G93A} mice injected at 45 days with the AAV-scFvD3H5 vector exhibited 28% more motor neurons in the lumbar spinal cord than the vehicle-injected SOD1^{G93A} mice (38.67 ± 0.67 per hemi section in AAV-scFvD3H5–treated mice versus 27.67 ± 2.19 in vehicle-treated mice, $P = 0.0086$) (Figure 7b).

Progressive axonal degeneration is also a hallmark of mutant SOD1 expression in transgenic mice.[28] Transverse sections from the L5 ventral root of AAV-scFvD3H5– and vehicle-injected SOD1^{G93A} mice at 120 days of age were collected and analyzed for the number of myelinated axons (Figure 7c). In sections from AAV-scFvD3H5–treated SOD1^{G93A} mice, 30% more myelinated axons were detected when compared with sections from vehicle-treated SOD1^{G93A} mice (Figure 7d) (582.3 ± 57.75 versus

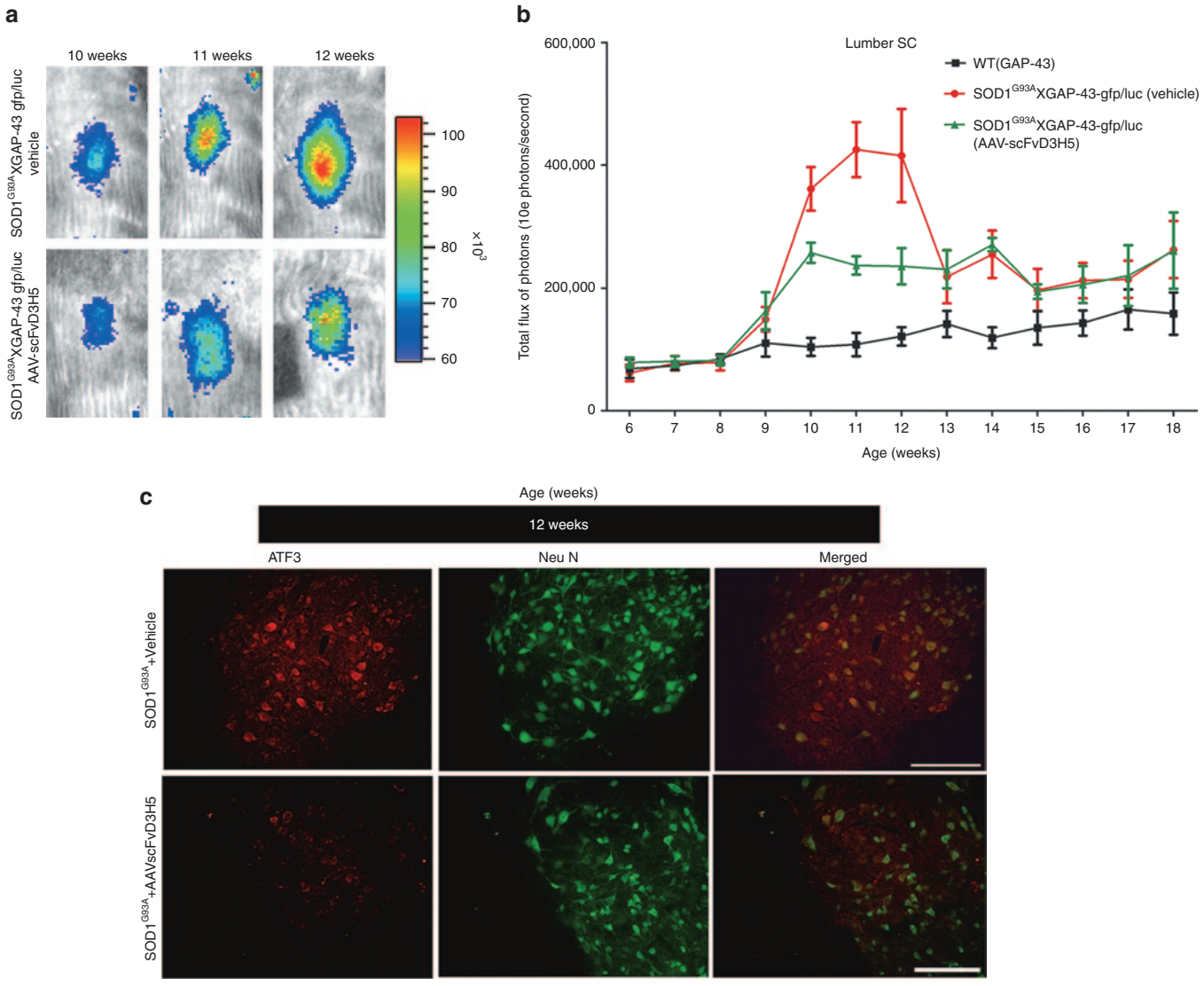

Figure 5. AAV-mediated delivery of scFvD3H5 antibody in GAP-43-luc/gfp;SOD1^{G93A} mice reduced neuronal stress. (**a**) *In vivo* bioluminescence imaging of GAP-43 induction was analyzed at various time points in spinal cord of GAP-43-luc/gfp;SOD1^{G93A} mice. Typical sequence of representative images of spinal cord area obtained from double-transgenic mice after AAV-scFvD3H5 or vehicle injection at different time points (10, 11, and 12 weeks) by *in vivo* imaging ($n = 6$ in each group) are shown. (**b**) Longitudinal quantitative analysis of total photon GAP-43 signal of bioluminescence in GAP-43-luc/gfp;SOD1^{G93A} mice in spinal cord is shown. Two-way ANOVA revealed a statistically significant reduction in neuronal stress between treated and untreated group at 11 and 12 weeks ($P < 0.05$). Error bar represents mean ± SEM. (**c**) Immunofluorescence using activating transcription factor 3 (ATF3, a marker for neuronal stress) and NeuN antibody was performed in spinal cord of AAV-scFvD3H5 mice and vehicle-treated mice at 12 weeks of age. ATF3 signal was found to be comparatively less in treated mice than in nontreated mice. Merging of both signals shows colocalization in motor neurons of spinal cord ventral horn. Scale bar 50 µm. AAV, adeno-associated virus; GFP, green fluorescent protein; scFv, single-chain fragment variable; SOD1, superoxide dismutase 1.

407.0 ± 10.12) in AAV-scFvD3H5–treated and vehicle-treated mice, respectively $P = 0.0403$).

DISCUSSION

Here, we report the testing of a novel gene therapy approach for ALS based on AAV delivery of recombinant secretable scFv antibody specific to misfolded SOD1 species. This secretable scFv antibody was derived as described below from a hybridoma cell line expressing a monoclonal antibody called D3H5, which is specific to misfolded SOD1.[16] A single intrathecal injection of AAV-scFvD3H5 in SOD1^{G93A} mice at 45 days of age yielded sustained expression of scFv molecules in the spinal cord. The treatment extended survival by an average of 16 days and by up to 40 days in direct correlation with the levels of antibody detected in tissue. It is also noteworthy that the approach succeeded in delaying disease onset and in attenuating gliosis.

Recent studies reported that intrathecal injection of AAV vectors yielded strong levels of biodistribution and motor neuron transduction in the spinal cord.[19] Here we tested this method to achieve high level and sustained production of secretable scFv antibodies in the spinal cord. Our results show that 5 weeks after single intrathecal injection of AAV-scFvD3H5 into SOD1^{G93A} mice, there was widespread immunodetection of scFv antibodies throughout the spinal cord including within ChAT-positive motor

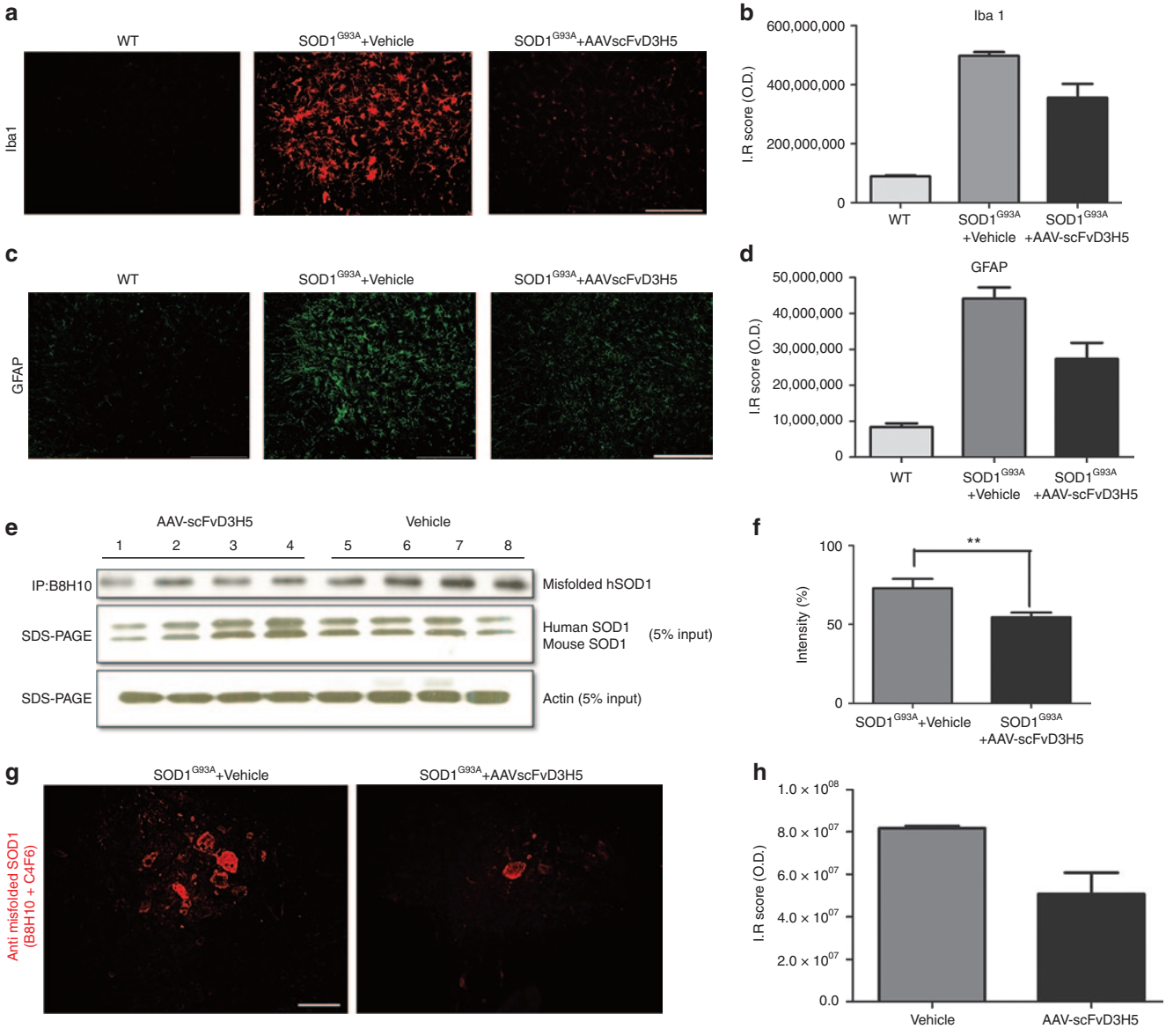

Figure 6. AAV-scFvD3H5 treatment resulted in decreased glial activation and reduced the burden of misfolded SOD1 in SOD1^{G93A} mice. (**a**) Lumbar spinal cord section from wild-type (WT) mice, SOD1^{G93A} mice treated with vehicle (middle), and SOD1^{G93A} mice treated with AAV-scFvD3H5 (right) as stained with anti-Iba1 antibody. (**b**) Quantification of immunoreactivity score for Iba1 showed statistically significant reduction of Iba1 signals in treated mice compared with untreated (n = 3 for each group; $P < 0.05$). (**c**) Representative pictures of glial fibrillary acidic protein (GFAP) immunofluorescence in the anterior horn of spinal cord from WT mice, SOD1^{G93A} control (middle), and AAV-scFvD3H5–treated SOD1^{G93A} (right). (**d**) The graph represents immunoreactivity quantification for GFAP, which was statistically reduced in treated mice. (n = 3 for each group). Data are mean ± SEM for all quantification (scale bar, 50 µm for all images). (**e**) Reduced level of misfolded SOD1 in the spinal cord of SOD1^{G93A} mice treated with AAV vector. (**f**) Intrathecal injection of AAV-scFvD3H5 led to reduction of ~19% in the levels of misfolded SOD1 species as detected by B8H10 antibody (P = 0.0293). Equal amount of proteins was used as shown on western blots after sodium dodecyl sulfate-polyacrylamide gel electrophoresis with an actin antibody. Commercial SOD100 polyclonal antibody revealed equal amount of SOD1 protein in all samples. Data represent the mean ± SEM. The P value was derived from Student's t-test. All images are from postnatal day 120 mice. (**g**) Representative pictures for immunofluorescence detection in spinal cord sections of misfolded SOD1 species with C4F6 and B8H10 antibodies. (**h**) Quantification of immunoreactivity score for misfolded SOD1 protein showed significant reduction of signal intensity in SOD1^{G93A} mice treated with AAV vector (n = 3 for each group; $P < 0.05$; scale bar 50 µm). AAV, adeno-associated virus; scFv, single-chain fragment variable; SOD1, superoxide dismutase 1.

neurons (**Figure 2**). The expression of scFv antibodies was persistent until end stage of disease, as revealed by anti-myc immunofluorescence and ELISA (**Figure 2**). We noticed variation in scFv antibody titers in the spinal cord from one mouse to another (**Figure 3e**), **a** phenomenon due in part to inherent technical difficulty to inject intrathecally in a small animal constant amount of AAV vectors. Nonetheless, the data revealed that longevity of SOD1^{G93A} mice correlated directly with the scFv antibody titer measured by ELISA in whole spinal cord lysates at end stage of disease. It is noteworthy that this immunotherapy approach via AAV delivery system extended survival of SOD1^{G93A} mice by up to 40 days. This would rank among the best therapeutic interventions accomplished so far in this mouse model of ALS with high copy number of mutant SOD1 transgene. There is also a recent

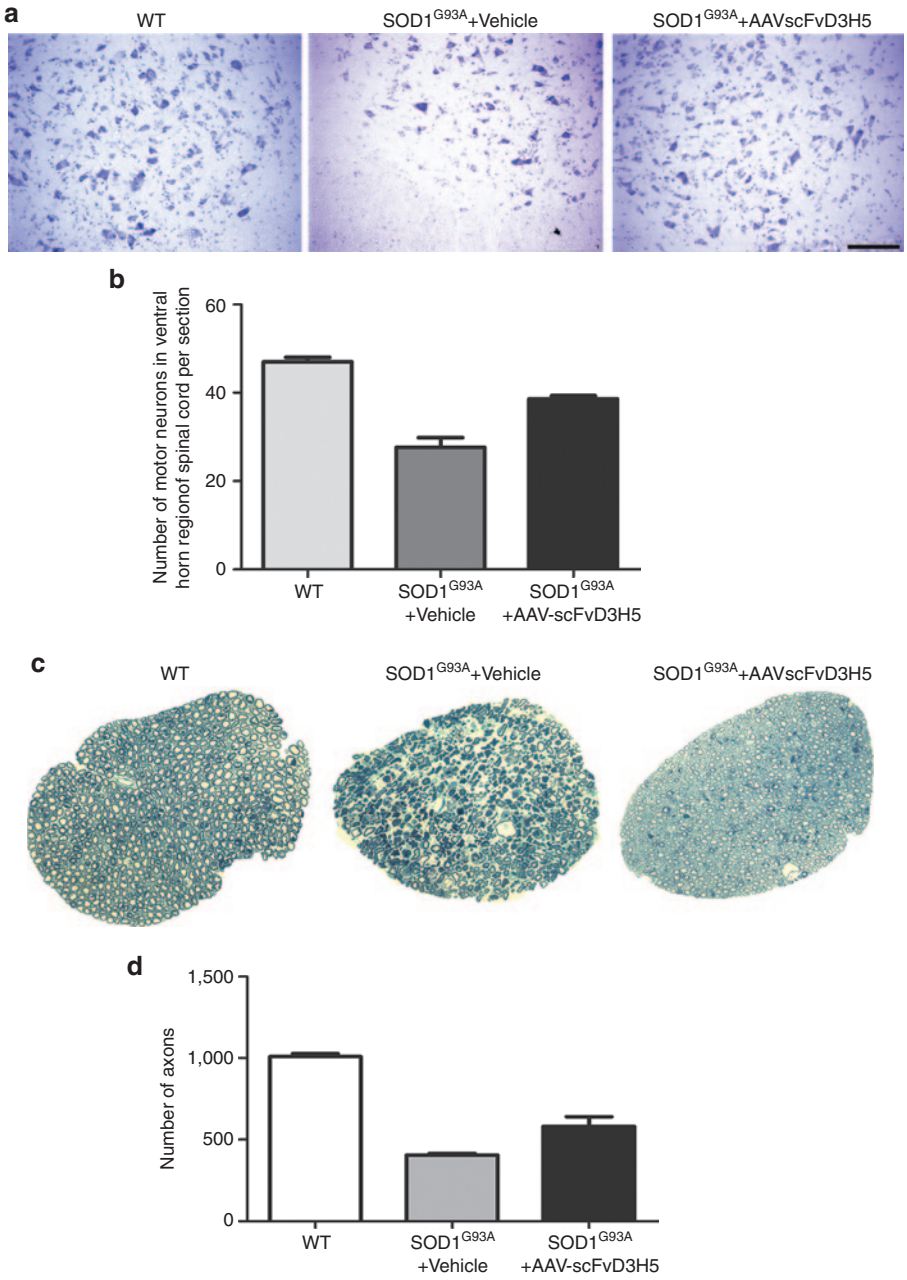

Figure 7. AAV-scFvD3H5 attenuated loss of motor neurons and ventral root axons in SOD1^{G93A} mice. (**a**) Cross-sections of cresyl violet stained hemi-lumbar spinal cord in wild-type (WT) mice, control SOD1^{G93A} mice, and AAV-scFvD3H5 mice at postnatal day 120 (P120). (**b**) AAV-scFvD3H5–treated SOD1^{G93A} mice contained 28% more motor neurons (38.6±0.6687; n = 3; P = 0.0086) compared with vehicle-treated SOD1^{G93A} mice (26.67±2.186; n = 3). Data are mean ± SEM. (**c**) Representative cross-section pictures of ventral roots of spinal cord lumbar segment from WT mice, control SOD1^{G93A} mice, and AAV-scFvD3H5 mice at P120. (**d**) Quantification of myelinated axons in the ventral root of spinal cord is shown. The total number of myelinated axons in control SOD1^{G93A} mice (407.0±10.12) was ~30% less compared with that in AAV-scFvD3H5–treated mice(582.3±57.75; P = 0.0203; n = 3 each group). Data are mean ± SEM. scFv, single-chain fragment variable; SOD1, superoxide dismutase 1.

report that AAV9 delivery of short hairpin RNA in SOD1^{G93A} mice to suppress SOD1 expression was similarly effective in conferring protection.[29] It should be noted that knocking down SOD1 levels in astrocytes from sporadic ALS was also found to attenuate astrocyte-mediated toxicity to motor neurons.[30] Nonetheless, an immunotherapeutic approach to target misfolded SOD1 species is more selective than short hairpin RNA approach[29] or an antisense oligonucleotide therapy, which aims to reduce messenger RNA levels encoding both mutant SOD1 and WT SOD1.[31]

The success of this therapeutic strategy lies in the fact that scFv antibodies are targeting misfolded SOD1 species, the source of toxicity in the disease.[32–34] Immunoprecipitation experiments from spinal cord lysates at end stage of disease mice confirmed that treatment led to a reduction in amount of misfolded SOD1 species (**Figure 6e**). The results also suggest a direct beneficial effect of scFv immunotherapy antibody on motor neurons. Bioimaging analysis of GAP-43/luc/gfp; SOD1^{G93A} mice treated with AAV-scFvD3H5 revealed reduction of neuronal stress at

presymptomatic stage (**Figure 5**). Symptoms monitoring also indicated a postponing of disease onset in SOD1^{G93A} mice injected with AAV-scFvD3H5 (**Figure 3c–e**). Such alleviation of motor neuron damage by scFvD3H5 antibody associated with delayed disease onset is consistent with previous studies on genetic ablation of mutant SOD1 within various cell types, which concluded that toxicity of mutant SOD1 exerted within motor neurons constitute a primary determinant of disease onset.[35]

A common characteristic of ALS is the occurrence of a neuroinflammatory reaction consisting of activated glial cells, mainly microglia and astrocytes. Previous studies have demonstrated that activated microglia induces the production of neurotoxic factors such as superoxide, nitric oxide, and proinflammatory cytokines, whereas reactive astrocytes express inflammatory markers such as iNOS.[36–38] It is now well established that the surrounding cells are active players in motor neuron dysfunction and death in mouse model of ALS as well as in familial ALS and sporadic ALS.[39,40] Here, the scFv treatment succeeded in attenuating the activation of microglia and astrocytes in the spinal cord of SOD1^{G93A} mice (**Figure 6a**,**b**), an effect that may contribute to neuroprotection.

These results suggest that AAV-based delivery of scFv antibodies against misfolded SOD1 species should be considered for treatment of ALS patients bearing SOD1 mutations. Unlike other drugs that act on deleterious pathways or cell survival, such immunotherapy-based approach can target specifically misfolded SOD1 species, the primary cause of toxicity in the disease. Moreover, there is evidence that aggregated forms of SOD1 can seed misfolding and aggregation of native WT SOD1 protein[41–43] Thus, the beneficial effects of antibodies might come not only from clearance of pathogenic SOD1 molecules but also from neutralization of toxic epitope exposed by misfolded SOD1 or from interference in formation and propagation of misfolded SOD1 species.[43] Moreover, another advantage of the AAV delivery approach is that it can achieve high level and sustained expression of secreted scFv antibodies without repeated injections of antibodies. Finally, the small size of scFv antibodies lacking Fc fragment allows them to thoroughly penetrate CNS tissues without adverse immune system response. It should be noted that secreted scFv antibodies may confer beneficial effects not only through binding of extracellular misfolded SOD1 but also through binding of intracellular SOD1 species as a previous study provided evidence of internalization of antibodies within motor neurons.[16] Here, scFv antibodies were detected in subsets of motor neurons (**Figure 2**).

An immunotherapy based on intrathecal inoculation of AAV to transduce in the CNS secretable scFv antibodies against misfolded SOD1 would be applicable for treatment of human ALS. Recombinant AAV vectors are vehicles of choice for gene transfer in the nervous system.[17,44] AAV can provide stable and safe gene expression with minimal immune responses. In recent years, AAV delivery of genes has been used with success in treatment of human genetic disorders, especially in retinal disease.[18,45] When injected into the CSF, AAV vectors can confer widespread and sustained transgene expression in the CNS.[17,19] Intrathecal injection in human ALS patients would require less AAV vectors than systemic injection and it would target production of scFv antibodies to the CNS, an immunoprivileged location. In the gene therapy approach described here, the question of what CNS cell types express the scFv antibody is not of crucial importance because the scFv protein has been engineered with an immunoglobulin secretion signal. The crucial point in this approach is the amount of scFv antibodies being secreted in the spinal cord milieu to maximize the benefits. As shown in **Figure 3**, there is a direct correlation between the amount of scFv antibodies in the spinal cord milieu and therapeutic effects. Thus, the transduction of secretable scFv molecules in various CNS cell types would be advantageous to achieve high levels of scFv antibodies in the milieu. Here, we have targeted through intrathecal injection expression of scFv antibodies to the CNS. There is no evidence that a peripheral sink for misfolded SOD1 would be beneficial as in Alzheimer's disease. An active immunization approach in SOD1^{G93A} mice failed to delay onset of disease and to delay survival,[15] whereas passive immunization based on intracerebroventricular infusion of anti-misfolded SOD1 antibody[16] or AAV-mediated delivery of scFv antibodies as shown here succeeded in conferred therapeutic effects.

An AAV-based immunotherapy to target misfolded SOD1 would be applicable for treatment of ALS patients carrying SOD1 mutations. A prophylactic treatment would even be conceivable for individuals carrying ALS-linked SOD1 mutations since the approach is capable to delay the onset of disease. Moreover, potential application of such immunotherapy to subsets of sporadic ALS cases cannot be excluded at this time as recent studies suggest the existence of misfolded/aggregated forms of SOD1 in sporadic ALS cases with no SOD1 mutations.[10,11,46,47]

METHODS

Generation of recombinant scFvD3H5 antibody. Messenger RNA was isolated from D3H5 hybridoma cell line[16] using a messenger RNA isolation kit (Qiagen, Chatsworth, CA). cDNA was synthesized using Superscript First Strand, catalog no. 12371-019 (Invitrogen,Carlsbad, CA) with oligodT priming according to the manufacturer's instructions. The variable regions of heavy chain (VH) and light chain (Vκ) were amplified separately from first-strand cDNA by using a mixture of universal polymerase chain reaction (PCR) primers and Platinum Pfx DNA polymerase (Invitrogen). The PCR products for heavy chain and light chain were cut with restriction enzymes *Pst*I/*Bst*EII and SacI/XhoI, respectively and agarose gel-purified. The cDNA inserts corresponding to VL and VH were cloned into the pBZUT7 vector and sequenced using M13 forward primer 5′-GTAAAACGACGCCCAG-3′ and reverse primer 5′-CAGGAAACAGCTATGAC-3′. The VH and VL domains were assembled and linked together by PCR to yield the full-length scFv gene. The scFv gene that was constructed in a VH-linker-VL format together with a standard flexible 20-amino acid linker (Gly4Ser)3 was then subcloned upstream of the Myc-tagged Psw1 scFVD1.3 Tag1 expression vector to generate scFvD3H5. Each scFv contained a murine immunoglobulin (Ig) κ-secretory signal for efficient secretion and a human c-myc epitope to facilitate detection (**Figure 1b**).

Expression and secretion of scFv vector in cultured cells. HEK293 cells were cultured in Dulbecco's modified Eagle's medium. The plasmids were transiently transfected with Lipofectamine (Invitrogen) into cells. After 48 hours, cells were harvested, and culture media was collected, centrifuged at 15,000*g* for 15 minutes at 4 °C, and the proteins in the media and cells were separated by 14% SDS-PAGE. After electrotransfer to polyvinylidene difluoride membranes (Immobilon-P, Millipore, Bedford, MA), scFvs were visualized by an HRP-conjugated anti-myc antibody (Invitrogen).

ScFvD3H5 binding to SOD1. The D3H5 monoclonal antibody has been shown to be specific only for misfolded SOD1, and it does not detect WT SOD1.[16] Western blot analysis and ELISA were performed to evaluate the immunoreactivity of scFvD3H5 to SOD1. 14% SDS-PAGE was carried out with spinal cord lysates of SOD1^{G93A} mice. Culture media from HEK293 cells transfected with scFv construct was used as a primary antibody source. After electrotransfer to polyvinylidene difluoride membranes, scFvs were visualized with an anti-myc antibody (Invitrogen). For ELISA, plates were coated with 3 µg/ml of recombinant SOD1^{G93A} protein. The harvested culture media was added at different dilutions to the coated plates and incubated at 4 °C overnight. On the next day, wells were washed and incubated with anti-myc-HRP antibody for 1 hour at room temperature to detect the scFv.

AAV-scFvD3H5 construction and preparation. The AAV serotype-2/1 vector (AAV2 terminal repeats in AAV1 capsids) encoding misfolded SOD1-scFv was prepared by standard method.[48] Briefly, to generate an AAV viral vector capable of conferring the capacity to produce and secrete the mAbD3H5 scFv upon infection, the fragment encompassing the scFv expression cassette in pScFvD3H5 was excised using HindIII and EcoRV and cloned into the plasmid BluescriptII KS(+) (Stratagene, Canada). It was then recloned as a SalI/NotI fragment into the XhoI/NotI digested plasmid AAV-CMV-GFP[49] replacing the EGFP-encoding sequence and creating the pscAAV-D3H5 plasmid to be used in the production of AAV recombinant viruses. For the production of scAAV recombinant viruses, the 293T cell line was used. Cells were cultured in Dulbecco's modified Eagle's medium (Gibco, Canada) supplemented with 10% normal bovine serum, 100 U/ml of penicillin G, and 100 µg/ml of streptomycin. Plasmids used for cotransfection of 293T cells were an ITR-containing plasmid derived from scAAV-CMV-GFP containing a scFv-encoding transgene (AAV-scFv or AAV-D1.3) and plasmids pXR1 and pxx-6 as packaging and helper plasmids, respectively[48,49]

Generation of GAP-43-luc/gfp; SOD1^{G93A} transgenic mice. Transgenic mice overexpressing SOD1^{G93A} mutations (B6SJL-TgN_ [SOD1-G93A] _1 Gur) were purchased from the Jackson Laboratory (Bar Harbor, ME) and were genotyped in accordance with Jackson Laboratory protocols. To confirm that the transgene copy number of SOD1^{G93A} was not altered in the mice used for this study, we evaluated genomic SOD1 levels by quantitative real-time PCR using genomic DNA isolated from tail tissue. Analysis of the mouse housekeeping gene encoding glyceraldehyde-3-phosphate dehydrogenase was used for normalization purposes. Oligoprimer pairs (used at concentration of 300 nm) were designed by GeneTool 2.0 software (Biotools, Edmonton, AB), and their specificity was verified by blast in the GenBank database. Standard cycling conditions were used.

Mice were maintained heterozygous in the C57BL/6 background. The transgenic GAP-43-luc/gfp reporter mice were generated as described previously.[23] These mice were crossed with the SOD1^{G93A} transgenic mice (C57/BL6, Jackson labs) to generate double-transgenic GAP-43-luc/gfp/SOD1^{G93A} mice. To avoid the effects of genetic background, all experiments were performed on age-matched littermates. Double-transgenic mice were genotyped according to the following procedure. The presence of GAP-43-luc/gfp transgene was assessed by PCR of the luciferase reporter gene with the following primers: 5′-GGCGCAGTAGGCAAGGTGGT and 5′-CAGCAGGATGCTCTCCAGTTC as described previously[21] The transgenic TLR2-LUC-AcGFP mice were generated and genotyped as described previously[21] The presence of the SOD1-G93A mutant transgene was assessed by PCR as previously described.[50] The use and maintenance of the mice described in this article was performed in accordance to the Guide of Care and Use of Experimental Animals of the Canadian Council on Animal Care.

In vivo *bioluminescence imaging.* As previously described, images were gathered using IVIS 200 Imaging System (Xenogen, Alameda, CA).[21] Twenty minutes before imaging session, the mice received intraperitoneal injection of D-luciferine, a luciferase substrate (150 mg/kg; Xenogen) dissolved in 0.9% saline. The mice were then anesthetized with 2% isoflurane in 100% oxygen at a flow rate of 2 l/ min and placed in the heated, light-tight imaging chamber. Images were collected using high-sensitivity charge-coupled device camera with wavelengths ranging from 300 to 600 nm. Exposition time for imaging was 1 minute using different field of views and F/1 lens aperture. The bioluminescence emission was normalized and displayed in physical units of surface radiance, photons per second per centimeter squared per steradian (photons/second/cm^2/sr). The light output was quantified by determining the total number of photons emitted per second using the Living Image 2.5 acquisition and imaging software (Xenogen). Region of interest measurements on the images were used to convert surface radiance (photons/s/cm^2/sr) to source flux or total flux of photons expressed in photons/second. Three-dimensional images were created using diffuse luminescent imaging tomography algorithms to reconstruct for the position, geometry, and strength of the internal light sources. The modifiable parameters were analyzed across the wavelengths, source spectrum, and tissue properties (Living Image 3D Analysis Software, Xenogen).

Intrathecal injection of AAV-scFvD3H5 in SOD1^{G93A} mice. Intrathecal injection of AAV-scFvD3H5 vector of vehicle in SOD1^{G93A} mice or GAP-43-luc/gfp/SOD1^{G93A} mice was carried out at postnatal day 45. A total of 3×10^9 particles were injected in a 10 µl volume by a Hamilton syringe, which was slipped under the dura, and the vector was slowly released into the CSF. The syringe was removed after 1 minute to minimize CSF and vector leakage. For all surgeries, mice were anesthetized with 2% isoflurane and posttreated with subcutaneous buprenorphine (0.05 mg/kg) for pain. As a control, age-matched SOD1^{G93A} mice received either same amount of vehicle or AAV vector encoding a lysozyme-specific single-chain fragment D1.3 (AAV-scFvD1.3) (n = 20 for all groups). After surgery, animals were housed in cage with free access to food and water till end point.

Analysis of disease progression. The onset of weight loss was determined as the time when mice started to exhibit a decline of body weight after reaching a peak value. The survival was defined as the age when the animal could not stand on feet within 30 seconds when placed on its side. Measurements of body weight, hind-limb reflex, and rotarod performance were used to score the clinical effects of SOD1^{G93A} mice. The extensibility and postural reflex of the hind limbs when mice were held up with their tails were scored as described previously.[12] The SOD1^{G93A} reflex score and body weight were measured every 2 days, beginning at 90 days. Scoring was performed in a blind manner by animal technicians who had no information about the genotype but had experience in grading SOD1^{G93A} mice paralysis. Analysis of SOD1^{G93A} mice disease progression was performed with an accelerated rotarod, starting at 4 rpm with a 0.25 rpm/second acceleration, and time was noted when the mice fell off the roll. Three trials were done per animal, and the mean value was calculated for statistics and graphs. Rotarod tests for SOD1^{G93A} mice were performed once a week.

ELISA for determining scFvD3H5 titer. The levels of scFvD3H5 in the spinal cord lysate were determined by ELISA. Spinal cord tissues were homogenized in lysis buffer (137×10^{-3} mol/l NaCl, 20×10^{-3} mol/l Tris (pH 8.0), 1% NP40, and 10% glycerol), supplemented with Protease Inhibitor Cocktail Tablets Complete Mini (Roche Applied Science, Laval, Quebec), ultrasonicated, and then centrifuged at 4 °C for 15 min at 8,000g. The supernatant was diluted in bicarbonate/carbonate coating buffer, and 100 µl of that was used to coat the 96-well ELISA plate (Peprotech, Dollard des Ormeaux, Quebec) overnight at 4 °C, followed by washing and blocking overnight again. The plates were then incubated sequentially with biotinylated 9E10 to c-myc (Abcam, Cambridge, MA) overnight, washed followed by incubation in streptividin-HRP (BD Pharmingen, Canada) for 1 hour at room temperature, and washed again followed by incubation in tetramethylbenzidine solution for color development. The reaction was

stopped with hydrochloric acid, and the absorbance at 450 nm was read. Spinal cord lysates from vehicle-injected mice were used as a control.

Immunoprecipitation and western blotting. At the end point, the spinal cord was dissected out, rapidly frozen in liquid nitrogen and stored at −80 °C for ELISA, immunoprecipitation, and western blot analysis. Whole protein lysates from spinal cord were extracted by homogenization of the tissues in TNG-T lysis buffer (50 mmol/l Tris-HCl pH: 7.4; 100 mmol/l NaCl; 10% glycerol; and 1% Triton X) and centrifugation for 20 minutes at 9,000*g* at 4 °C. The soluble protein was quantified by the Lowry method. Immunoprecipitation of misfolded SOD1 was performed as previously described.[16] Briefly, beads were coated with mouse monoclonal anti-misfolded SOD1 antibody B8H10 for immunoprecipitating misfolded SOD1 and incubated overnight with whole spinal cord lysate, washed, and fractioned on 14% SDS-PAGE. Immunoprecipitation of spinal cord extracts expressing scFvD3H5 was performed by immunoprecipitating with anti c-myc tag as described earlier.[20]

Immunohistochemistry. Mice were anesthetized by intraperitoneal injection of 4% chloral hydrate and perfused intracardially with phosphate-buffered saline, followed by 4% paraformaldehyde, pH 7.4. Spinals cords were removed, postfixed for 1 hour, frozen in Tissue-Tek OCT embedding compound (Sakura Finetek, Torrance, CA), permeabilized in 0.25% Triton-X for 10 minutes, blocked in 3% normal goat serum for 1 hour, and then incubated with the monoclonal antibodies for 16 hours at 20 °C. Sections were then incubated overnight at 20 °C using primary antibodies, such as 1:100 mouse monoclonal anti-myc 9E10 (Abcam), 1:250 rabbit ChAT (Millipore), 1:500 rabbit polyclonal anti-GFAP (Dako, Carpinteria, CA), 1:500 rabbit anti-Iba1 (Wako Chemicals, Richmond, VA), 1:50 rabbit polyclonal ATF3 (Santa Cruz Biotechnology, Santa Cruz, CA), 1:500 mouse monoclonal NEU N (Millipore, Temecula, CA), and 1:100 mouse monoclonal B8H10 and C4F6 (Medimabs, Montreal, Canada).Visualization was made by incubating the slides with Alexa-Fluors 488 or 594 rabbit anti-mouse secondary antibody (Invitrogen). Dissected dorsal root ganglia were postfixed in a solution of 3% glutaraldehyde for a period of 48 hours, washed in phosphate-buffered saline, treated with 1% osmium tetra oxide for 2 hours, and dehydrated through graded alcohol solutions. Before Epon plastic embedding, dorsal root ganglia were further dissected to ensure that all ventral root axons would be sampled at a distance of 3 mm from the dorsal root ganglia cell body. Semi-thin cross-sections were stained with toluidine blue, rinsed, and cover slipped. To quantify the immunoreactivity score of immunofluorescent sections, we measured the optical densities of each staining with ImageJ software (NIH, Bethesda, MD).

Statistical analyses. Data were analyzed using Prism 5.0 software (GraphPad Software, LaJolla, CA). Behavioral data were computed by performing two-way ANOVAs (except when specified) followed by Bonferroni posttests and survival data using Mantel-Cox log-rank tests. Ventral root axon counts and immunoreactivity scores for Iba1, GFAP, and anti-misfolded SOD1-specific antibody were compared using two-tailed Student's *t*-tests. Data are expressed as mean ± SEM. $P < 0.05$ was considered statistically significant.

SUPPLEMENTARY MATERIAL

Figure S1. Real-time imaging of TLR2 induction after LPS/AAV-scFvD3H5 or AAV-svFvD1.3 injection in TLR2-LUC-AcGFP transgenic mice.

Figure S2. Longitudinal quantsitative analysis of total photon GAP-43 signal/bioluminescence in GAP-43-luc/gfp/SOD1G93A double-transgenic mice and WT mice in spinal cord.

ACKNOWLEDGMENTS

We gratefully thank Sophie Vachon for her technical help. This work was supported by the Canadian Institutes of Health Research, Prionet Canada, the Amyotrophic Lateral Sclerosis Society of Canada, and the Robert Packard Center for ALS Research at Johns Hopkins. J.-P.J. holds a Canada Research Chair Tier 1 in mechanisms of neurodegeneration. J.K. holds a Senior Scholarship from Fonds de recherche du Québec en Santé.

REFERENCES

1. Tandan, R and Bradley, WG (1985). Amyotrophic lateral sclerosis: part 2. Etiopathogenesis. *Ann Neurol* **18**: 419–431.
2. Gurney, ME (1994). Transgenic-mouse model of amyotrophic lateral sclerosis. *N Engl J Med* **331**: 1721–1722.
3. Pramatarova, A, Figlewicz, DA, Krizus, A, Han, FY, Ceballos-Picot, I, Nicole, A *et al.* (1995). Identification of new mutations in the Cu/Zn superoxide dismutase gene of patients with familial amyotrophic lateral sclerosis. *Am J Hum Genet* **56**: 592–596.
4. Eisen, A, Mezei, MM, Stewart, HG, Fabros, M, Gibson, G and Andersen, PM (2008). SOD1 gene mutations in ALS patients from British Columbia, Canada: clinical features, neurophysiology and ethical issues in management. *Amyotroph Lateral Scler* **9**: 108–119.
5. Reaume, AG, Elliott, JL, Hoffman, EK, Kowall, NW, Ferrante, RJ, Siwek, DF *et al.* (1996). Motor neurons in Cu/Zn superoxide dismutase-deficient mice develop normally but exhibit enhanced cell death after axonal injury. *Nat Genet* **13**: 43–47.
6. Bruijn, LI, Miller, TM and Cleveland, DW (2004). Unraveling the mechanisms involved in motor neuron degeneration in ALS. *Annu Rev Neurosci* **27**: 723–749.
7. Ezzi, SA, Urushitani, M and Julien, JP (2007). Wild-type superoxide dismutase acquires binding and toxic properties of ALS-linked mutant forms through oxidation. *J Neurochem* **102**: 170–178.
8. Gruzman, A, Wood, WL, Alpert, E, Prasad, MD, Miller, RG, Rothstein, JD *et al.* (2007). Common molecular signature in SOD1 for both sporadic and familial amyotrophic lateral sclerosis. *Proc Natl Acad Sci USA* **104**: 12524–12529.
9. Kabashi, E, Valdmanis, PN, Dion, P and Rouleau, GA (2007). Oxidized/misfolded superoxide dismutase-1: the cause of all amyotrophic lateral sclerosis? *Ann Neurol* **62**: 553–559.
10. Bosco, DA, Morfini, G, Karabacak, NM, Song, Y, Gros-Louis, F, Pasinelli, P *et al.* (2010). Wild-type and mutant SOD1 share an aberrant conformation and a common pathogenic pathway in ALS. *Nat Neurosci* **13**: 1396–1403.
11. Pokrishevsky, E, Grad, LI, Yousefi, M, Wang, J, Mackenzie, IR and Cashman, NR (2012). Aberrant localization of FUS and TDP43 is associated with misfolding of SOD1 in amyotrophic lateral sclerosis. *PLoS ONE* **7**: e35050.
12. Urushitani, M, Sik, A, Sakurai, T, Nukina, N, Takahashi, R and Julien, JP (2006). Chromogranin-mediated secretion of mutant superoxide dismutase proteins linked to amyotrophic lateral sclerosis. *Nat Neurosci* **9**: 108–118.
13. Urushitani, M, Ezzi, SA and Julien, JP (2007). Therapeutic effects of immunization with mutant superoxide dismutase in mice models of amyotrophic lateral sclerosis. *Proc Natl Acad Sci USA* **104**: 2495–2500.
14. Takeuchi, S, Fujiwara, N, Ido, A, Oono, M, Takeuchi, Y, Tateno, M *et al.* (2010). Induction of protective immunity by vaccination with wild-type apo superoxide dismutase 1 in mutant SOD1 transgenic mice. *J Neuropathol Exp Neurol* **69**: 1044–1056.
15. Liu, HN, Tjostheim, S, Dasilva, K, Taylor, D, Zhao, B, Rakhit, R *et al.* (2012). Targeting of monomer/misfolded SOD1 as a therapeutic strategy for amyotrophic lateral sclerosis. *J Neurosci* **32**: 8791–8799.
16. Gros-Louis, F, Soucy, G, Larivière, R and Julien, JP (2010). Intracerebroventricular infusion of monoclonal antibody or its derived Fab fragment against misfolded forms of SOD1 mutant delays mortality in a mouse model of ALS. *J Neurochem* **113**: 1188–1199.
17. Towne, C, Schneider, BL, Kieran, D, Redmond, DE Jr and Aebischer, P (2010). Efficient transduction of non-human primate motor neurons after intramuscular delivery of recombinant AAV serotype 6. *Gene Ther* **17**: 141–146.
18. Bennicelli, J, Wright, JF, Komaromy, A, Jacobs, JB, Hauck, B, Zelenaia, O *et al.* (2008). Reversal of blindness in animal models of leber congenital amaurosis using optimized AAV2-mediated gene transfer. *Mol Ther* **16**: 458–465.
19. Snyder, BR, Gray, SJ, Quach, ET, Huang, JW, Leung, CH, Samulski, RJ *et al.* (2011). Comparison of adeno-associated viral vector serotypes for spinal cord and motor neuron gene delivery. *Hum Gene Ther* **22**: 1129–1135.
20. Wuertzer, CA, Sullivan, MA, Qiu, X and Federoff, HJ (2008). CNS delivery of vectored prion-specific single-chain antibodies delays disease onset. *Mol Ther* **16**: 481–486.
21. Lalancette-Hébert, M, Phaneuf, D, Soucy, G, Weng, YC and Kriz, J (2009). Live imaging of Toll-like receptor 2 response in cerebral ischaemia reveals a role of olfactory bulb microglia as modulators of inflammation. *Brain* **132**(Pt 4): 940–954.
22. Saxena, S, Cabuy, E and Caroni, P (2009). A role for motoneuron subtype-selective ER stress in disease manifestations of FALS mice. *Nat Neurosci* **12**: 627–636.
23. Gravel, M, Weng, YC and Kriz, J (2011). Model system for live imaging of neuronal responses to injury and repair. *Mol Imaging* **10**: 434–445.
24. Perrin, FE, Boisset, G, Docquier, M, Schaad, O, Descombes, P and Kato, AC (2005). No widespread induction of cell death genes occurs in pure motoneurons in an amyotrophic lateral sclerosis mouse model. *Hum Mol Genet* **14**: 3309–3320.
25. Nascimento, D, Pozza, DH, Castro-Lopes, JM and Neto, FL (2011). Neuronal injury marker ATF-3 is induced in primary afferent neurons of monoarthritic rats. *Neurosignals* **19**: 210–221.
26. Fischer, LR, Culver, DG, Tennant, P, Davis, AA, Wang, M, Castellano-Sanchez, A *et al.* (2004). Amyotrophic lateral sclerosis is a distal axonopathy: evidence in mice and man. *Exp Neurol* **185**: 232–240.
27. Pasinelli, P and Brown, RH (2006). Molecular biology of amyotrophic lateral sclerosis: insights from genetics. *Nat Rev Neurosci* **7**: 710–723.
28. Zhang, B, Tu, P, Abtahian, F, Trojanowski, JQ and Lee, VM (1997). Neurofilaments and orthograde transport are reduced in ventral root axons of transgenic mice that express human SOD1 with a G93A mutation. *J Cell Biol* **139**: 1307–1315.
29. Foust, KD, Salazar, DL, Likhite, S, Ferraiuolo, L, Ditsworth, D, Ilieva, H *et al.* (2013). Therapeutic AAV9-mediated suppression of mutant SOD1 slows disease progression and extends survival in models of inherited ALS. *Mol Ther*; published online 15 September 2013.

30. Haidet-Phillips, AM, Hester, ME, Miranda, CJ, Meyer, K, Braun, L, Frakes, A *et al.* (2011). Astrocytes from familial and sporadic ALS patients are toxic to motor neurons. *Nat Biotechnol* **29**: 824–828.
31. Smith, RA, Miller, TM, Yamanaka, K, Monia, BP, Condon, TP, Hung, G *et al.* (2006). Antisense oligonucleotide therapy for neurodegenerative disease. *J Clin Invest* **116**: 2290–2296.
32. Bruijn, LI, Houseweart, MK, Kato, S, Anderson, KL, Anderson, SD, Ohama, E *et al.* (1998). Aggregation and motor neuron toxicity of an ALS-linked SOD1 mutant independent from wild-type SOD1. *Science* **281**: 1851–1854.
33. Bruijn, LI, Becher, MW, Lee, MK, Anderson, KL, Jenkins, NA, Copeland, NG *et al.* (1997). ALS-linked SOD1 mutant G85R mediates damage to astrocytes and promotes rapidly progressive disease with SOD1-containing inclusions. *Neuron* **18**: 327–338.
34. Wang, J, Farr, GW, Hall, DH, Li, F, Furtak, K, Dreier, L *et al.* (2009). An ALS-linked mutant SOD1 produces a locomotor defect associated with aggregation and synaptic dysfunction when expressed in neurons of Caenorhabditis elegans. *PLoS Genet* **5**: e1000350.
35. Boillée, S, Yamanaka, K, Lobsiger, CS, Copeland, NG, Jenkins, NA, Kassiotis, G *et al.* (2006). Onset and progression in inherited ALS determined by motor neurons and microglia. *Science* **312**: 1389–1392.
36. Barbeito, LH, Pehar, M, Cassina, P, Vargas, MR, Peluffo, H, Viera, L *et al.* (2004). A role for astrocytes in motor neuron loss in amyotrophic lateral sclerosis. *Brain Res Brain Res Rev* **47**: 263–274.
37. Block, ML, Zecca, L and Hong, JS (2007). Microglia-mediated neurotoxicity: uncovering the molecular mechanisms. *Nat Rev Neurosci* **8**: 57–69.
38. Moisse, K and Strong, MJ (2006). Innate immunity in amyotrophic lateral sclerosis. *Biochim Biophys Acta* **1762**: 1083–1093.
39. Clement, AM, Nguyen, MD, Roberts, EA, Garcia, ML, Boillée, S, Rule, M *et al.* (2003). Wild-type nonneuronal cells extend survival of SOD1 mutant motor neurons in ALS mice. *Science* **302**: 113–117.
40. Yamanaka, K, Boillee, S, Roberts, EA, Garcia, ML, McAlonis-Downes, M, Mikse, OR *et al.* (2008). Mutant SOD1 in cell types other than motor neurons and oligodendrocytes accelerates onset of disease in ALS mice. *Proc Natl Acad Sci USA* **105**: 7594–7599.
41. Chia, R, Tattum, MH, Jones, S, Collinge, J, Fisher, EM and Jackson, GS (2010). Superoxide dismutase 1 and tgSOD1 mouse spinal cord seed fibrils, suggesting a propagative cell death mechanism in amyotrophic lateral sclerosis. *PLoS ONE* **5**: e10627.
42. Münch, C and Bertolotti, A (2011). Self-propagation and transmission of misfolded mutant SOD1: prion or prion-like phenomenon? *Cell Cycle* **10**: 1711.
43. Grad, LI, Guest, WC, Yanai, A, Pokrishevsky, E, O'Neill, MA, Gibbs, E *et al.* (2011). Intermolecular transmission of superoxide dismutase 1 misfolding in living cells. *Proc Natl Acad Sci USA* **108**: 16398–16403.
44. Samaranch, L, Salegio, EA, San Sebastian, W, Kells, AP, Foust, KD, Bringas, JR *et al.* (2012). Adeno-associated virus serotype 9 transduction in the central nervous system of nonhuman primates. *Hum Gene Ther* **23**: 382–389.
45. Maguire, AM, Simonelli, F, Pierce, EA, Pugh, EN Jr, Mingozzi, F, Bennicelli, J *et al.* (2008). Safety and efficacy of gene transfer for Leber's congenital amaurosis. *N Engl J Med* **358**: 2240–2248.
46. Forsberg, K, Jonsson, PA, Andersen, PM, Bergemalm, D, Graffmo, KS, Hultdin, M *et al.* (2010). Novel antibodies reveal inclusions containing non-native SOD1 in sporadic ALS patients. *PLoS ONE* **5**: e11552.
47. Guareschi, S, Cova, E, Cereda, C, Ceroni, M, Donetti, E, Bosco, DA *et al.* (2012). An over-oxidized form of superoxide dismutase found in sporadic amyotrophic lateral sclerosis with bulbar onset shares a toxic mechanism with mutant SOD1. *Proc Natl Acad Sci USA* **109**: 5074–5079.
48. Rabinowitz, JE, Rolling, F, Li, C, Conrath, H, Xiao, W, Xiao, X *et al.* (2002). Cross-packaging of a single adeno-associated virus (AAV) type 2 vector genome into multiple AAV serotypes enables transduction with broad specificity. *J Virol* **76**: 791–801.
49. McCarty, DM, Monahan, PE and Samulski, RJ (2001). Self-complementary recombinant adeno-associated virus (scAAV) vectors promote efficient transduction independently of DNA synthesis. *Gene Ther* **8**: 1248–1254.
50. Gowing, G, Dequen, F, Soucy, G and Julien, JP (2006). Absence of tumor necrosis factor-alpha does not affect motor neuron disease caused by superoxide dismutase 1 mutations. *J Neurosci* **26**: 11397–11402.